Downloaded from jnm.snmjournals.org by on March 14, 2017. For personal use only.

Role of Lipid-Soluble Complexes in Targeted Tumor Therapy

Mathew L. Thakur, PhD[1,2]; Ron Coss, PhD[2]; Roger Howell, PhD[3]; Donka Vassileva-Belnikolovska, MD[4]; Jeff Liu, BS[1]; Sampath P. Rao, PhD[1]; Greg Spana, BS[1]; Phyllis Wachsberger, PhD[2]; and Dennis L. Leeper, PhD[2]

[1]Department of Radiology, Thomas Jefferson University, Philadelphia, Pennsylvania; [2]Department of Radiation Oncology, Thomas Jefferson University, Philadelphia, Pennsylvania; [3]University of Medicine and Dentistry of New Jersey, Newark, New Jersey; and [4]National Center of Clinical and Transfusional Haematology, Sofia, Bulgaria

Radionuclide therapy remains a promising arsenal against cancer. However, low tumor uptake, high radiation dose to normal organs, and subsequent adverse effects are challenging problems. This study assessed the therapeutic significance of lipid-soluble compounds of ^{111}In, which passively diffuse through the cell membrane, bind to cytoplasmic components, and remain cell bound until decay. **Methods:** Athymic nude mice bearing human colorectal, prostate, or breast cancer received 11.1–14.8 MBq (300–400 μCi) ^{111}In-8-hydroxyquinoline (^{111}In-oxine) or ^{111}In-mercaptopyridine-*N*-oxide (^{111}In-Merc) in 200 μL solution intratumorally through a multihole needle. Tumors in some mice were dissected, and 20-μm-thick sections were autoradiographed. In additional mice, tumor diameter was measured daily, mice were imaged and weighed, and blood samples were drawn for determination of neutrophil counts for up to 28 d after injection. Some mice were sacrificed at predetermined times for quantitative tissue distribution of ^{111}In. Additionally, tumor cells were labeled with ^{111}In-oxine and homogenized, and ^{111}In associated with cell components was determined using polyacrylamide gel electrophoresis. Radiation dose that could be delivered to adjacent tissues was estimated. The ^{111}In absorbed dose as a function of radial position *r* in a 1-g tumor was theoretically compared with those of β-emitting radionuclides ^{90}Y and ^{177}Lu. **Results:** More than 85% of ^{111}In remained in tumors, bound to cell cytoplasmic components of apparent molecular weights 250 and 6 kDa. ^{111}In in tumors was uniformly distributed. Only 2% of the injected ^{111}In was in the liver, kidneys, and carcass. Statistical analysis showed that on day 28, control tumors grew >100%, whereas treated tumors either had growth arrest or grew only slowly (17%). The estimated radiation dose per megabecquerel (millicurie) injected was 90 Gy/g (9,000 rad/g), of which 64% was from conversion electrons, 16% from Auger electrons, 20% from γ-photons and x-rays, respectively. Radiation dose to adjacent normal organs was 5%–10% of the radiation dose to the tumor and negligible to the liver and kidneys. Neutrophil counts remained unchanged. Mouse body weight was ±10% of the initial weight. The radiation dosimetry for ^{111}In and ^{177}Lu compared favorably, but not that of ^{90}Y. **Conclusion:** Treatment is independent of receptor density, heterogeneity, or the hypoxic status of cells. It is applicable to treat all known and accessible tumor types, and it delivers a negligible radiation dose to vital organs and only 5%–10% of the radiation dose to organs adjacent to the tumor. Intratumoral administration of ^{111}In-oxine appears to be a feasible, effective, safe, and promising treatment for cancer.

Key Words: targeted radionuclide therapy

J Nucl Med 2003; 44:1293–1300

Every 10 s, there is 1 cancer-related death in the United States alone (*1*). The primary treatment against cancer remains surgery, chemotherapy, radiation therapy, and radionuclide therapy. Treatments on the horizon are vaccine therapy that spurs the immune system, gene therapy that introduces genes to eradicate malignant cells, and targeted drug therapy that is designed to take advantage of certain specific receptors that are overexpressed on tumor cells. Although the surgical removal of tumors followed by therapeutic intervention is the mainstay of cancer management, not all tumors can be radically or even partially dissected without serious consequences that can severely degrade the quality of the patient's life (*2*). Brachytherapy, in which radioactive seeds are implanted, may not deliver a uniform radiation dose and is supplemented by external radiation therapy (*3*,*4*). With external-beam radiation therapy, the dose to the surrounding normal tissues could be high, and therapy could be less effective if the tumor is hypoxic (*3*). Failure of local therapy is considered a source of new and distant metastases and, subsequently, mortality (*5*). Clinically significant risks associated with radio- or chemotherapy are neutropenia, thrombocytopenia, nausea, skin burn, and hair loss. In the case of systemically introduced radionuclide therapy, there is also concern regarding excessive radiation dose to the normal, healthy organs.

We hypothesize that a radionuclide with suitable physical and chemical characteristics that will distribute uniformly within the tumor and bind to cell cytoplasmic components until completely decayed will deliver a high radiation dose to the tumor cell nucleus, eventually leading to cell death, while sparing normal tissue. Such a treatment, in principle, is desirable, and may be more effective, and safer than the

Received Jan. 10, 2003; revision accepted Apr. 21, 2003.
For correspondence or reprints contact: Mathew L. Thakur, PhD, Thomas Jefferson University, 1020 Locust St., Suite 359JAH, Philadelphia, PA 19107.
E-mail: Mathew.Thakur@mail.tju.edu

Downloaded from jnm.snmjournals.org by on March 14, 2017. For personal use only.

current treatments by which patients with tumors that are too risky to resect or cannot be radically extirpated are managed. Such radionuclide therapy should also be applicable to most solid tumors and metastatic lesions, such as those in the liver, lungs, or brain.

We have prepared the 2 lipid-soluble chelates of ^{111}In—namely, ^{111}In-8-hydroxyquinoline (^{111}In-oxine) and ^{111}In-mercaptopyridine-*N*-oxide (^{111}In-Merc) (*6–8*). When in contact with cells, the agents passively diffuse through the cell membrane and ^{111}In forms strong complexes with the cytoplasmic components (*9,10*). The protein-bound ^{111}In then remains within the cell. Because of this characteristic, ^{111}In-oxine has been used for decades to label human neutrophils, platelets, lymphocytes, tumor-infiltrated lymphocytes, lymphokine-activated killer cells, and dendritic cells with diagnostically useful quantities of ^{111}In (*11–19*). Using ^{111}In-oxine to label human lymphocytes, ten Berge et al. and McLean et al. were able to demonstrate extensive chromosomal aberrations (*20–22*). Rao et al. also showed that ^{111}In-oxine was highly radiotoxic to spermatogonial cells (*23*). Recently, Fortin et al. have reported that local treatment of tumors with radiotherapy not only inhibits cancer cell proliferation but also prevents metastatic transformation (*5*).

For the most effective treatment of a tumor using such an agent, it will be necessary that the agent be injected within the tumor and the solution be homogeneously distributed to most, if not all, of the cells. Ultrasound or fluoroscopic guidance techniques have made precise needle insertions routinely feasible, which could be applied for intratumoral injection of these agents. Because of this possibility, intratumoral injections are gaining popularity, even in chemotherapy (*24*) and antisense gene therapy (*25*). The purpose of this communication is to present preliminary findings and discuss the advantages as well as the limitations of such a technique.

MATERIALS AND METHODS

^{111}In-Lipid–Soluble Agents

^{111}In-Oxine was either obtained from Mallinckrodt (Tyco International) pharmacy or prepared using the method of Thakur et al. from ^{111}In-chloride solution purchased from Nordion (*6*). ^{111}In-Merc was also prepared using the method of Thakur et al. (*7*). These were taken up in a sterile solution containing ~10% EtOH in 0.9% NaCl. The specific activity for each preparation was rendered 55.5–74 MBq/mL (1.5–2.0 mCi/mL).

Cell Culture and Labeling

To determine that the technique is not specific for any type of cancer, we implanted in athymic nude mice 3 different types of human tumors. Human prostate cell line DU145, human colorectal cancer cell line LS174T, and human breast cancer cell line T47D were obtained from the American Type Culture Collection and cultured in a suitable medium at 37°C in a humidified incubator containing 5% CO_2/95% air. Confluent cells were harvested by standard tissue culture techniques and suspended in culture medium, and cell concentration was determined using a hemocytometer and a light microscope.

To determine that the ^{111}In-oxine labels tumor cells, just as it does human peripheral blood cells, DU145 cells were suspended in *N*-(2-hydroxyethyl)piperazine-*N*′-(2-ethanesulfonic acid) (HEPES) buffer containing ^{111}In-oxine and incubated at 22°C for 10 min. Cells were then centrifuged, resuspended in culture medium, and carefully spread on collagen-plated glass slides. The slides were allowed to dry, autoradiographed using Kodak emulsion, and photographed.

Intracellular Location of ^{111}In in DU145 Human Prostate Tumor Cells

Cell Preparation. Although these lipid-soluble complexes are known to label blood cells and ^{111}In translocates to cytoplasmic components (*9,10*), we wanted to ascertain in vitro that ^{111}In-oxine (a) can label DU145 human prostate tumor cells chosen as a tumor model, (b) binds to proteins within the cells, and (c) once bound, remains bound to proteins.

DU145 cells were grown in exponential growth (~3×10^7 per T-75 flask) in Dulbecco's modification of Eagle medium (DMEM) at 37°C in 5% CO_2/95% air. Cells were washed twice with 10 mL sterile HEPES buffer (25 mmol/L) in 0.75% NaCl. To each flask was added 4.7 MBq (127 μCi) ^{111}In-oxine in 4 mL HEPES buffer; flasks were closed, placed on a gentle shaker in a 37°C walk-in room, and incubated for 90 min. The cells were then collected, centrifuged at 450*g* × 5 min, and washed once with Hank's balanced salt solution; the radioactivity associated with the cells and that remaining in the supernatant combined with the wash was measured. Cells were resuspended in DMEM, reseeded separately in 3 fresh T-75 flasks, and treated as follows at 2, 24, and 48 h later.

Still floating, cells in the 2-h flask (flask A) were centrifuged at 450*g* × 5 min and washed with HEPES buffer. More than 90% of the radioactivity was associated with the cells processed as described below. In the 24-h (flask B) and 48-h (flask C) flasks, many cells had attached and had grown nearly to confluency. The medium from each flask was collected, flasks were gently rinsed with 5 mL HEPES buffer, and the wash was combined with the supernatant medium and centrifuged. The radioactivity in the supernatant and that remaining in the cells were measured. The total activity removed from flask B was 46.6%, of which 83.3% was cell associated. In flask C, 57.7% was removed, and 83.1% was cell associated.

Polyacrylamide Gel Analysis. Cells from flask A and those retained and attached in flasks B and C were then solubilized in 1 mL lysis buffer consisting of 0.0625 mol/L Tris HCl, 10% glycerol, 10% sodium dodecyl sulfate (SDS), 40 mmol/L dithiothreitol, 1 mmol/L ethylenediaminetetraacetic acid, and the following antiproteases: 14 mg/L aprotinin, 0.7 mg/L pepstatin, and 5 mmol/L phenylmethylsulfonylfluoride. The resulting viscous solution was pipeted into a 2-mL conical centrifuge tube and heated in a boiling water bath for 7 min. The 2- and 24-h cell digests were then frozen at −80°C until the 48-h cell digest was prepared. Protein concentration was determined using a Bio-Rad Bradford assay and Beckman DU640 spectrophotometer. The cell digest containing 15 μg protein was then loaded onto Bio-Rad 12% polyacrylamide minigels in duplicate, mixed with 10 μmol/L bromphenol blue dye. At either end of the wells on the gels, a standard molecular weight marker mixture was also loaded. Polyacrylamide (12%)/SDS gels were made with 3% stacking gels using a 30% acrylamide/bisacrylamide solution. Gels were run in a Novex X cell II minigel system at 90 V until the dye reached the gel/stacking interface and

Downloaded from jnm.snmjournals.org by on March 14, 2017. For personal use only.

then at 200 V until the dye front reached the bottom of the gel. The running buffer consisted of 0.025 mol/L Trizma (tris) base, 0.192 mol/L glycine, and 0.1% SDS. Gels run in duplicate were then removed and washed in water. For visualization of protein bands, 1 gel was stained with GelCode blue, destained, washed in water, dried, and wrapped in plastic wrap.

The other gel was exposed for 96 h to a high-resolution phosphor imaging plate and analyzed using Fuji Film's BAS-5000 high-resolution phosphor IV scanner. The percentage of the radioactivity in 3 protein bands in each lane was calculated.

Distribution of ^{111}In in Tumors in Mice

DU145 tumors were grown to ~1 cm in diameter in the right thigh of 5 athymic nude mice weighing between 19 and 22 g. A 20-gauge multihole needle was designed and fabricated in our workshop. Approximately 0.74–3.33 MBq (20–90 μCi) ^{111}In-oxine were drawn into a 1-mL syringe (0.1–0.2 mL), and the solution was slowly injected after inserting the multihole needle only at 1 site, horizontally into the tumor. The needle was withdrawn and light pressure was applied on the needle hole to prevent any solution oozing out of the tumor. Four hours later, mice were sacrificed, and tumors were excised, measured for radioactivity, and quickly frozen using Histoprep tissue embedding media and Histofreeze refrigerant spray (Fisher Scientific). Several 20-μm-thick sections were cut perpendicular to the needle insertion, collected on glass slides, and autoradiographed. Sections were then stained with hematoxylin and eosin, observed under a microscope for viable and necrotic cells, and photographed.

For comparison, ^{111}In-oxine was injected in some tumor-bearing mice with a regular, 20-gauge, "end-hole" needle, and tumor samples were processed as above.

Experiments in Nude Mice Bearing Human Tumors

Approximately 5×10^6, viable human prostate (DU145), breast (T47D), or colorectal cancer (LS174T) cells were implanted in nude mice in groups of 10 mice each, and tumors were allowed to grow to ~0.5 cm in diameter. Approximately 18.5 MBq (500 μCi) ^{111}In-oxine or ^{111}In-Merc in 100 μL of 10% EtOH in isotonic saline were injected per tumor (n = 10 each) with a 20-gauge multihole needle. The initial (day 1) tumor size in each group of mice was different, because it was dependent on the number of days that had elapsed between the xenografts day and the day of the experiment. Control mice (n = 10 each) received the solution without ^{111}In or with decayed ^{111}In. Daily, tumor diameter was measured, the mice were weighed, and radioactivity retained in the animal body was measured in a Capintec CRC-10 dose calibrator. Periodically, the mice were imaged using a General Electric 300 STARCAM gamma camera equipped with a parallel-hole collimator and a dedicated computer. Mice were sacrificed 2 or 3 wk later to determine quantitative distribution of radioactivity and for tissue histology. Tumor diameter was measured with a Vernier caliper (Fowler) in 3 different places in tumors. To minimize day-to-day variations in measurements, readings were obtained by the same individual. Mice bearing human breast cancer T47D tumors were given ^{111}In-Merc similarly and followed as described.

Means and SDs were calculated for mice tumor data (2 groups of 10 mice each × 3 daily readings per tumor × 21 d [excluding weekends] = 1,260 observations). These data were plotted as a function of days for both groups. The percentage increase from day 1 to day 28 was calculated. Three-way ANOVA of tumor size (group by day by subjects nested within group) with a group-by-day interaction term was performed. Pairwise comparisons of tumor size on the day of measurement were analyzed with Bonferroni t tests. Two-way ANOVAs were conducted within both groups to test whether there was a change in tumor size by the day of measurement within each group.

Determination of Hematologic Toxicity

During the treatment of cancer with systematically induced chemo- or radiotherapeutic agents, neutropenia is a common adverse reaction. To assess the polymorphonuclear leukocyte (PMN) status during the course of ^{111}In treatment, the following procedure was performed.

Two days before injecting ^{111}In-oxine or ^{111}In-Merc, the tumor-bearing mice were placed in a ventilated acrylic box in such a way that the tail of the animal was easily accessible, while the rest of the body remained in the box. The tail vein was then gently punctured with a 27-gauge sterile needle and a drop of blood was allowed to form, which was smeared on a glass slide and stained with Wright's stain. At least 100 white cells were counted under a light microscope, and the percentage of PMNs in the total number of white cells counted was determined. This served as the base PMN concentration. The procedure was then performed daily for 28 d after the mice were treated, each with 16.7 MBq (450 μCi) ^{111}In-oxine. Results were calculated as the percentage of PMNs as a function of time after injection. All animal protocols were approved by the American Association of Laboratory Animal Care–licensed institutional Animal Care and Use Committee.

Calculations for Radiation Dose to Tumor and Adjacent Normal Organs

For a 1-g tumor containing 10^9 cells, 37-MBq (1 mCi) intratumoral injection results in an average of 13,028 decays per cell after >10 half-lives have elapsed. Thus, an absorbed dose of 17.55 Gy (1,755 rad) was obtained, which represents the self-dose to the cell (*26*). The cell, however, is located within a cluster of similarly labeled cells and, therefore, the cross-dose from energetic conversion electrons, γ-rays, and x-rays must be considered. In fact, the multicellular dosimetry calculations of Goddu et al. (*27*) show that, under conditions where the cells are uniformly labeled, the cross-dose from ^{111}In is far greater than the self-dose and, therefore, the average absorbed dose to the tumor is more important.

Our calculations are based on the assumption that 37 MBq (1 mCi) ^{111}In will be uniformly distributed in a spheric tumor of mass 1 g (1.24 cm in diameter for unit density matter) and will undergo a complete decay with its physical half-life (T_p) of 67.9 h. The path lengths of the Auger electrons emitted by ^{111}In range from 0 to 8.6 μm, those of the conversion electrons are from 200 to 600 μm, and the mean free paths for the 2 γ-rays are approximately 6.5 and 8 cm, respectively (*28*,*29*). The techniques and computer code described by Howell et al. (*30*) were used to calculate the mean absorbed dose to the tumor as well as the dose profile across the tumor and in the surrounding healthy tissue. For comparison, these calculations were also performed for ^{177}Lu and ^{90}Y using the full radiation spectra, including β-spectra. These radionuclides have physical half-lives of 6.7 d and 64 h, respectively, and emit β-particles with maximum energies of 498 keV and 2,280 keV, respectively (*31*). The corresponding maximum ranges are 0.18 and 1 cm, respectively (*32*). The essence of these is given in the Results.

Downloaded from jnm.snmjournals.org by on March 14, 2017. For personal use only.

RESULTS

The labeling efficiencies of both ^{111}In-oxine and ^{111}In-Merc were >90%. ^{111}In-Oxine was used in most experiments because it was readily available. However, when concentrations of >37 MBq/mL (>1 mCi/mL) were required, it was prepared in our laboratory. Interest in Merc stemmed from its thermodynamic stability constants, which are higher (association constant [K_a] = 10^{12} vs. K_a = 10^8) than those of ^{111}In-oxine (*7*). As can be seen later in this section, however, both agents produced similar results.

When human prostate cancer cells DU145 were incubated with ^{111}In-oxine, >90% of the radioactivity was incorporated by the cells and was uniformly bound to the cells, as determined by microautoradiography followed by photography (Fig. 1).

When DU145 cells in culture were incubated with ^{111}In-oxine for 2, 24, and 48 h, the distribution of radioactivity in the cell lysate (Fig. 2) was remarkably similar. The results of radioactivity distribution between the cell lysates of flask A (0–2 h), flask B (24 h), and flask C (48 h) were also remarkably similar. In each case, 5% of the radioactivity was bound to protein of apparent molecular weight >250 kDa, 15% to apparent molecular weight of 22 kDa, and 38% to apparent molecular weight of 6 kDa. The radioactivity remaining was diffusely spread throughout the lane.

The distribution of radioactivity in mouse tumor, injected using a multihole needle, was distinctly different from that injected using a regular end-hole needle (Fig. 3). It was evident from the autoradiography that the radioactivity injected using the end-hole needle covered a small tumor area, only around the end-hole, whereas almost the entire tumor area was covered by the radioactivity injected through the multihole needle.

The tumors treated with nonradioactive placebo continued to grow, irrespective of their type—breast, prostate, or colorectal. Within 28 d after injection, the prostate tumors in placebo grew to nearly 100% of their initial size, whereas the tumors treated with 16.7 MBq (450 μCi) ^{111}In-oxine grew, on the average, only 17% (Fig. 4). Both increases appeared linear over days, but the slope for the control group was steeper than that for the treated group. The groups-by-day measurements are significant (<0.0001) for 2-way ANOVAs. The groups-by-day interaction term is significant in the 3-way ANOVA showing that the change over days is different for the 2 groups. Pairwise comparisons show that for the control group, most comparisons that are >1 measurement day apart are significantly different



FIGURE 1. Autoradiographic presentation of DU145 tumor cells labeled with ^{111}In-oxine. Cells were labeled in HEPES buffer, washed, spread on collagen-plated glass slides, autoradiographed using Kodak emulsion, and photographed. Intensely labeled cells are seen.

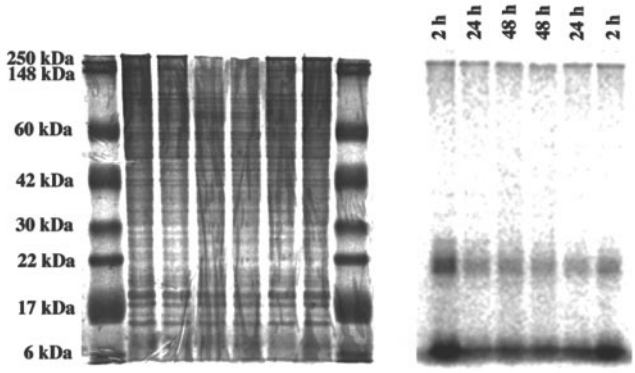


FIGURE 2. Composite of stained gel (left) and gel that was autoradiographed (right). Major portion of radioactivity (right) was associated with 3 protein bands of apparent molecular weights >250, 22, and 6 kDa. Irrespective of different time periods for which ^{111}In remained in cells (2, 24, or 48 h), neither distribution nor portion of ^{111}In bound to proteins was changed.

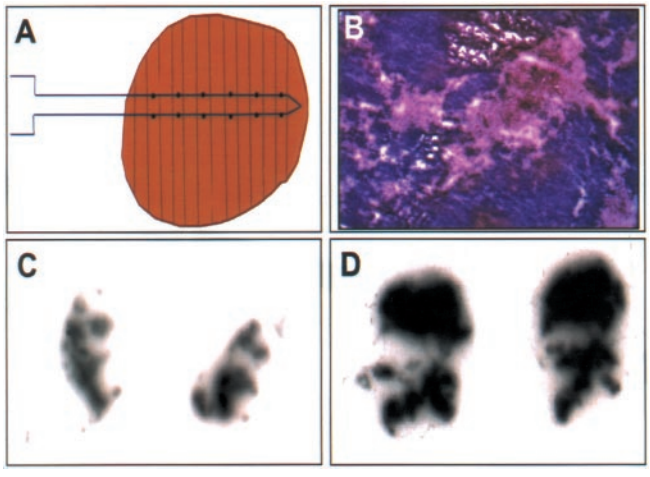


FIGURE 3. (A) Schematic diagram of tumor, needle, and sections of tumors cut in perpendicular to path of needle. Two autoradiographs show 2 separate 20-μm-thick sections of tumor into which ^{111}In was injected through sprinkler needle (D) and that of tumor that was injected with regular needle (C). Tumor injected with sprinkler needle has spread over larger portion of tumor than that injected with regular needle. Because of tumor necrosis (B), even with sprinkler needle, ^{111}In uptake in tumor is patchy and there is no ^{111}In in center. Necrotic tissue can be seen (lightly stained part) in histologic section of tumor (B).

Downloaded from jnm.snmjournals.org by on March 14, 2017. For personal use only.

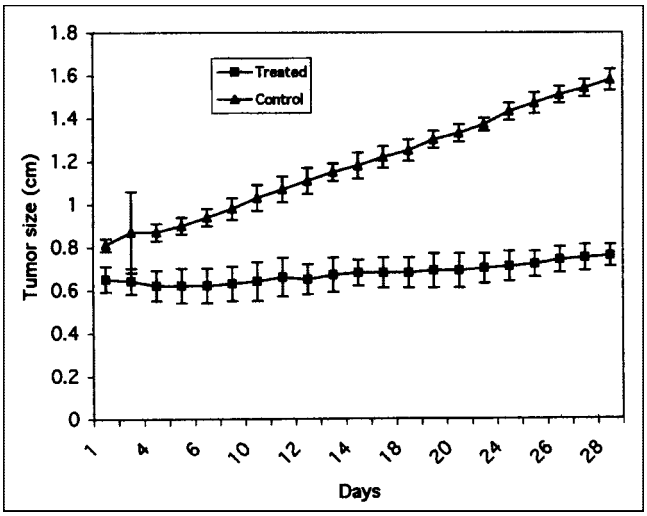


FIGURE 4. Tumor growth (diameter) as function of time in days after 2 groups of mice bearing experimental human prostate cancer DU145 each received ~16.7 MBq (~450 μCi) ^{111}In-oxine and other group, also bearing tumor, received only 10% EtOH solution in 0.9% NaCl. Dose received by tumors was ~42 Gy (~4,200 rad).

from each other, whereas, for the treated group, comparisons must generally be >3 d apart to be significant. Similarly, untreated breast tumors grew to nearly 500% of their initial size, whereas those injected with 13.3 MBq (360 μCi) ^{111}In-Merc ceased their growth in almost all tumors. The body weight of the mice remained ±10% of their initial weight.

At 22 d after injection, >85% of the administered radioactivity had remained in the tumor (Fig. 5). At this time, radioactivity in the kidneys and liver was 2% of the injected dose/g each and 2% had remained in the rest of the carcass. The radioactivity remaining was excreted in the urine within the first 24 h, as was evident by the daily whole-body radioactivity measurements. The bone marrow radioactivity was negligible. As a result, the white blood cell counts in all animals remained practically unchanged from the levels before the initiation of treatment.

The dosimetry program of Howell et al. (*30*) gives the mean absorbed dose per unit cumulated activity *S*. For 37 MBq (1 mCi) of ^{111}In uniformly distributed in a spheric tumor of 1 g, the values of *S* are 4.8×10^{-3} Gy/MBq-h (0.01811 rad/μCi-h) from γ- and x-rays (20% of total dose), 15.6×10^{-3} Gy/MBq-h (0.05776 rad/μCi-h) from conversion electrons (64% of total dose), and 4×10^{-3} Gy/MBq-h (0.01502 rad/μCi-h) from Auger electrons (16% of total dose), making a total of 24.5×10^{-3} Gy/MBq-h (0.0909 rad/μCi-h). The cumulated activity $\tilde{A}$ for a 37-MBq (1 mCi) intratumoral administration with no biologic clearance is $1.44\ A_o\ T_p = 1.44$ (37 MBq [1,000 μCi]) (67.9 h) = 9.778×10^4 μCi-h. Finally, the total mean absorbed dose to the 1-g tumor is $D = \tilde{A}\ S = 2.43$ Gy/MBq injected (9,000 rad/mCi injected). For many tumor cells, this dose is lethal (*22*).

The calculation above represents the mean absorbed dose to a static tumor (not growing or shrinking). If the tumor grows and subsequently shrinks during the decay of ^{111}In, then the absorbed dose calculations will require modification. If shrinkage is observed during the decay of ^{111}In, we can revise our dose estimates by taking into account the reduction in mass as a function of time after injection. This calculation is readily handled by the methods described by Howell et al. (*30*,*34*) and Goddu et al. (*33*).

The mean absorbed dose is 2.43 Gy/MBq (9,000 rad/mCi) ^{111}In injected. The dose profile across the tumor (Fig. 6) shows that the absorbed dose is somewhat higher at the center of the tumor (96.2 Gy [9,620 rad]) and drops off to about one half of that value at the periphery. In treating prostate cancer, for example, it is assumed that the bladder wall is about 0.1 cm from the edge of the tumor; this tissue receives a dose of only about 7 Gy (700 rad). If it is assumed that the rectal wall is 0.3 cm from the edge of the tumor, this tissue only receives a dose of about 4 Gy (400 rad). Therefore, the mean absorbed dose to the tumor is 10–20 times

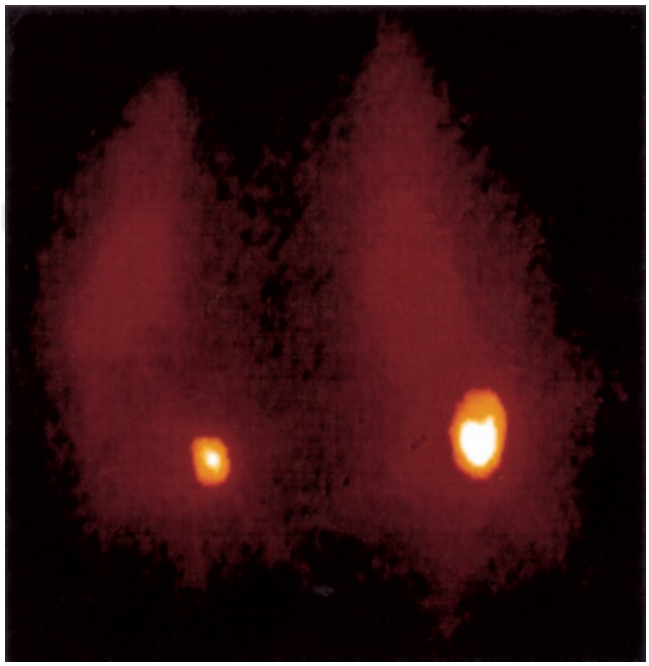


FIGURE 5. Composite of posterior images of 2 nude mice bearing human prostate tumor DU145. Twenty days earlier, mouse at left was given 12.6 MBq (340 μCi) ^{111}In-oxine and mouse on right was given 16.7 MBq (450 μCi) ^{111}In-Merc. Images show that >90% of ^{111}In is still in tumor (intense white spot). In either case, tumor size had not increased. At sacrifice, 93% of ^{111}In was still associated with tumor, ~2% was in kidneys, and 2% in liver. Remaining 2% was in carcass. Total amount of ^{111}In (corrected to decay) remaining in mice was 85% ± 3% of activity injected. Dose received by these tumors was estimated to be ~32 Gy (~3,200 rad) and ~42 Gy (4,200 rad), respectively. (Note that because of low resolution of gamma camera, it appears in these images that ^{111}In is homogeneously spread in tumor, including that in necrotic portion of tumor. In autoradiographs, Fig. 3, better resolution is achieved and absence of ^{111}In in necrotic area is visible.).

Downloaded from jnm.snmjournals.org by on March 14, 2017. For personal use only.

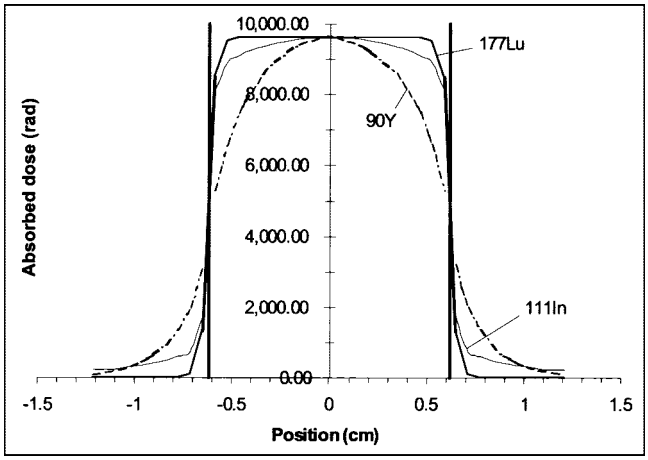


FIGURE 6. Absorbed dose as function of radial position r in 1-g tumor (diameter, 1.24 cm) containing 37 MBq (1 mCi) of uniformly distributed ^{111}In (thin solid line). Bold vertical lines denote boundaries between tumor ($-0.62 < r < 62$ cm) and normal tissue ($-1.5 < r < -0.62$ and $0.62 < r < 1.5$ cm). Note precipitous drop in absorbed dose as one moves from tumor to normal tissue. Calculations were performed using methods described by Howell et al. (*34*). Also shown are dose profiles for ^{177}Lu (bold solid line) and ^{90}Y (dashed line). Profiles for these radionuclides correspond to injected activities (4.67 MBq [0.126 mCi] and 2.22 MBq [0.060 mCi], respectively) that deliver, on complete decay, same dose to center of tumor as 37 MBq (1 mCi) ^{111}In (96.2 Gy [9,620 rad]).

higher than the dose to adjacent healthy tissues or the absorbed dose to the adjacent healthy organs is only 5%–10% of the dose to the tumor (Fig. 6). For the sake of comparison, also shown in Figure 6 are dose profiles for the β-particle emitters ^{177}Lu and ^{90}Y. Due to the high energy of the β-particles emitted by ^{90}Y, the dose profile is nonuniform within the 1-g tumor and relatively high doses are delivered to the bladder wall (20 Gy [2,000 rad]) and rectal wall (4.5 Gy [450 rad]). In contrast, the medium-energy β-emitting ^{177}Lu delivers a relatively uniform dose to the tumor and very low doses to the bladder wall (0.86 Gy [86 rad]) and rectal wall (0.07 Gy [7 rad]). Thus, the radiation dosimetry for ^{111}In and ^{177}Lu compares highly favorably with prostate brachytherapy, for example, in which radiation dose to the bladder and rectal wall are estimated to be 100% to that of the prostate tumor and to that of the external-beam therapy, in which, on the average, 25% of the bladder wall and 35% of the rectal wall receive 100% of the dose to the tumor (*35*).

DISCUSSION

^{111}In possesses physical characteristics that allow one to image its in vivo distribution externally by γ-imaging. ^{111}In also emits Auger electrons, conversion electrons, and x-rays. When ionic ^{111}In is converted into lipid-soluble compounds, administered directly into tumors in living mice, the chelate passively diffuses through the cell membrane and ^{111}In binds to cytoplasmic components and, thereby, provides a significant radiation dose to the cells. We estimate that when 37 MBq (1 mCi) ^{111}In is uniformly distributed into a 1-g tumor, the radiation dose is 90 Gy (9,000 rad) for complete decay of ^{111}In. Approximately 64% of this dose is due to conversion electrons, which have path ranges from 200 to 600 μm, which is equal to ~20–60 cells deep. These data suggest that even if ^{111}In is not in the nucleus of each cell, cytotoxicity to target cells is likely to be induced, as long as the radionuclide remains in the cells to which it is bound. Furthermore, once bound to cell cytoplasmic components, ^{111}In remains cell bound, does not redistribute (or only minimally redistributes, <10%), and, thereby, imparts only a negligible dose to healthy organs. Our experimental data substantiated the fact that the mice treated with ^{111}In lipid-soluble complexes neither had neutropenia nor did they lose significant body weight (<10%), while their tumor growth was either arrested or was negligible as compared with treated control tumors. It should be borne in mind that the quantity of ^{111}In we administered in this feasibility study was chosen arbitrarily and was not optimal to demonstrate its therapeutic effectiveness. Further studies that will lead us to administer a calculated quantity of ^{111}In that will induce cell kill are strongly warranted, as our data demonstrated that at 16.7 MBq (450 μCi) (~42 Gy [~4,200 rad]), the DU145 human prostate tumors continued to grow, albeit slowly, whereas the growth of T47D human breast tumors was arrested at only 13.3 MBq (360 μCi) ^{111}In (~32 Gy [~3,200 rad]).

The use of a multihole needle substantially improved the distribution of the injectate solution over the regular end-hole needle. Nonetheless, a formula must be worked out experimentally that will guide us to calculate the exact volume of injectate necessary to sufficiently cover the tumor of a given size. Tumor volume could be determined using a regular CT scan. Lipid-soluble ^{111}In solutions could be mixed with a predetermined quantity of contrast agents that, when injected, will allow physicians and surgeons to assess whether the solution injected had covered the entire tumor. An additional volume of the radioactivity solution could be injected if required.

Because this agent needs to be injected directly into the tumor or the portion of it that would not be safely extracted, the technique is limited to treat only known solid tumors and not unknown metastatic lesions. Nonetheless, this simple technique has numerous potential advantages over the current systemically given chemo- or radiotherapeutic agents, which induce substantial toxicity to normal, healthy organs and adversely affect the quality of the patient's life. Even as compared with brachytherapy or external-beam therapy, this technique promises to induce a significantly smaller radiation dose to tissues in the immediate vicinity of the target. Although our data are preliminary, they are consistent with our hypothesis. Furthermore, this approach is applicable to all tumors, including those that may be refractory to chemo- or radiotherapy.

Downloaded from jnm.snmjournals.org by on March 14, 2017. For personal use only.

Because ^{111}In is the radionuclide of therapeutic importance, the use of ^{111}In-Octreotide for the treatment of somatostatin receptor–positive tumors has been investigated (*36*,*37*). In this approach, at the present time, to treat even small tumors, up to 18.5 MBq (500 mCi) ^{111}In-Octreotide is intravenously administered. Besides the cost, high radiation dose to the kidneys is also a matter of concern. The present technique promises to be effective with a much smaller quantity than 18.5 MBq (500 mCi) and significantly less radiation dose to healthy organs. This postulation is consistent with our experimental data, which demonstrated no loss of circulating PMNs in treated mice and indicated the lack of toxic dose to the bone marrow. Although, because of practical difficulties we did not account for circulating blood platelets, it should be reasonable to predict from the PMN data that thrombocytopenia is also unlikely to occur. Furthermore, our theoretic calculations suggested that the radiation dose to normal organs adjacent to the tumor might also be negligible, as compared with external-beam therapy or interventions with any other forms of radionuclides.

As can be seen from our data, >80% of the administered dose remains in the tumor. Any ^{111}In-oxine ($K_a = 10^8$) that may escape into systemic circulation will bind to plasma transferrin or lactoferrin with $K_a = 10^{26}$ (*6*). ^{111}In bound to transferrin or lactoferrin clears rapidly via urinary excretion and minimizes radiation dose to the whole body or other normal tissues. This is an additional advantage of this radionuclide.

The list of lipid-soluble complexes of ^{111}In is not limited to ^{111}In-oxine. Other lipid-soluble complexes such as ^{111}In-Merc and ^{111}In-tropolone could be equally effective. We chose ^{111}In-oxine predominantly, not only because it is the one that is commercially available but also because the intracellular behavior of this compound is more thoroughly investigated than that of ^{111}In-Merc (*10*) or any other ^{111}In compound that can be used for this application. However, this targeted approach is not limited to either the use of ^{111}In or to its oxine, Merc, or tropolone complexes. Any other radionuclide of therapeutic importance chelated with any compound that could form a lipid-soluble complex with the radioactive metal ions would serve the purpose. For example, ^{177}Lu and ^{90}Y are possible candidates for this purpose. The dose profiles for these radionuclides in Figure 6 suggest that the energetic β-emitter ^{90}Y is not a good candidate for this approach. The medium-energy β-emitter ^{177}Lu does appear promising. However, for ^{177}Lu to be an effective therapeutic agent, the radionuclide, like ^{111}In, must remain cell bound and not egress out of the tumor. At the time of this writing, such characteristics of ^{177}Lu are unknown. Furthermore, the much smaller activities required for ^{177}Lu and its relatively low yield of γ-rays may limit the imaging capability of this radionuclide for these applications.

With promising efficacy, lower risk, and lower and relatively affordable cost of ^{111}In-oxine, we believe that this approach, although simplistic, can play a major role in targeted tumor therapy and is worthy of further investigation.

CONCLUSION

Our data, although preliminary, suggest that lipid-soluble complexes of ^{111}In injected directly into a tumor can deliver a high radiation dose and arrest tumor growth without excessive radiation dose to normal organs and adjacent tissues, weight loss, or bone marrow toxicity. Care must be taken, however, that the agent distribute uniformly within the tumor. The treatment can be effective, regardless of the tumor type, its receptor density, the receptor heterogeneity, the vascularity, its hypoxic status, or for those that may be refractory to chemotherapy.

ACKNOWLEDGMENTS

We are grateful to Lawrence Parker, PhD, Thomas Jefferson University, for his expertise in the biostatistical analysis of the animal data and to Christopher Storck for the preparation of Figure 2. We also thank Ms. Kate Musselman for the preparation of the manuscript. Support for this research was provided, in part, by the International Atomic Energy Agency.

REFERENCES

1. Brady LJ, Levit SH. Future directions of imaging research: subspecialty society messages. *Radiology.* 1998;209:593–596.
2. Sandler HM. Prostate cancer: patient's dilemma? *Cancer J Sci Am.* 1998;4:347–348.
3. Critz FA, Levinson AK, Williams WH, et al. Simultaneous radiotherapy for prostate cancer: ^{125}I prostate implant followed by external-beam radiation. *Cancer J Sci Am.* 1998;4:359–363.
4. McLaughlin PW, Narayana V, Fields MT, et al. Permanent implantation of I-125 sources in the prostate: radical limits of simplicity. *Radiology.* 1999;213:839–844.
5. Fortin A, Larochelle M, Laverdiere J, et al. Local failure is responsible for the decrease in survival for patients with breast cancer treated with conservative surgery and postoperative radiotherapy. *J Clin Oncol.* 1999;17:101–109.
6. Thakur ML, Coleman RE, Welch MJ. Indium-111-labeled leukocytes for the localization of abscesses: preparation, analysis, tissue distribution, and comparison with gallium-67 citrate in dogs. *J Lab Clin Med.* 1977;89:217–228.
7. Thakur ML, McKenney SL, Park CH. Simplified and efficient labeling of human platelets in plasma using indium-111–2-mercaptopyridine-N-oxide: preparation and evaluation. *J Nucl Med.* 1985;26:510–517.
8. Thakur ML, McKenney SL, Park CH. Evaluation of indium-111–2-mercaptopyridine-N-oxide for labeling leukocytes in plasma: a kit preparation. *J Nucl Med.* 1985;26:518–523.
9. Thakur ML, Segal AW, Louis L, et al. Indium-111-labeled cellular blood components: mechanism of labeling and intracellular location in human neutrophils. *J Nucl Med.* 1977;18:1022–1029.
10. Thakur ML, McKenney SL. Indium-111-mercaptopyridine-N-oxide-labeled human leukocytes and platelets: mechanism of labeling and intracellular location of ^{111}In and mercaptopyridine-N-oxide. *J Lab Clin Med.* 1986;107:141–147.
11. Thakur ML, Lavender JP, Arnot RN, et al. Indium-111-labeled autologous leukocytes in man. *J Nucl Med.* 1977;18:1014–1021.
12. Thakur ML, Walsh L, Malech HL, et al. Indium-111-labeled human platelets: improved method, efficacy, and evaluation. *J Nucl Med.* 1981;22:381–385.
13. Lavender JP, Goldman JM, Arnot RN, Thakur ML. Kinetics of indium-111 labeled lymphocytes in normal subjects and patients with Hodgkin's disease. *Br Med J.* 1977;2:797–799.
14. Thakur ML, Welch MJ, Joist H, et al. Indium-111 labeled platelets: studies on preparation and evaluation of in vitro and in vivo functions. *Thromb Res.* 1976;9:345–357.
15. Muul LM, Nason-Burchenal K, Carter CS, et al. Development of an automated

Downloaded from jnm.snmjournals.org by on March 14, 2017. For personal use only.

closed system for generation of human lymphokine-activated killer. *J Immunol Methods.* 1987;101:171–181.
16. Rosenberg SA, Lotze MT, Muul LM, et al. A new approach to the therapy of cancer based on the systemic administration of autologous lymphokine-activated killer cells and recombinant interleukin-2. *Surgery.* 1986;100:262–272.
17. Rosenberg SA, Lotze MT, Muul LM, et al. A progress report on the treatment of 157 patients with advanced cancer using lymphokine-activated killer cells and interleukin-2 or high-dose interleukin-2 alone. *N Engl J Med.* 1987;316:889–897.
18. Morse MA, Coleman RE, Akabani G, Niehaus N, Coleman D, Lyerly HK. Migration of human dendritic cells after injection in patients with metastatic malignancies. *Cancer Res.* 1999;59:56–58.
19. Eggert AAO, Schreurs MWJ, Boerman OC, et al. Biodistribution and vaccine efficiency of murine dendritic cells are dependent on the route of administration. *Cancer Res.* 1999;59:3340–3345.
20. ten Berge RJM, Natarajan AT, Hardeman MR, et al. Labeling with indium-111 has detrimental effects on human lymphocytes: concise communication. *J Nucl Med.* 1983;24:615–620.
21. McLean JR, Blakey DH, Douglas GR, et al. The Auger electron dosimetry of ^{111}In in mammalian cells *in vitro. Radiat Res.* 1989;119:205–210.
22. Thakur ML, McAfee JG. The significance of chromosomal aberrations in indium-111 labeled lymphocytes. *J Nucl Med.* 1984;25:922–927.
23. Rao DV, Sastry KSR, Grimmond HE, et al. Cytotoxicity of some indium radiopharmaceuticals in mouse testes. *J Nucl Med.* 1988;29:375–384.
24. Horton HM, Hernandez P, Parker SE, et al. Antitumor effect of interferon-ω: in vivo therapy of human tumor xenografts in nude mice. *Cancer Res.* 1999;59:4064–4068.
25. Mohan PM, Chintala SK, Mohanam S, et al. Adenovirus-mediated delivery of antisense gene to urokinase-type plasminogen activator receptor suppresses glioma invasion and tumor growth. *Cancer Res.* 1999;59:3369–3373.
26. Silvester DJ. Consequences of indium-111 decay in vivo: calculated absorbed radiation dose to cells labeled by indium-111-oxine. *J Labelled Compds Radiopharm.* 1978;19:196–197.
27. Goddu SM, Rao DV, Howell RW. Multicellular dosimetry for micrometastases: dependence of self-dose versus cross-dose to cell nuclei on type and energy of radiation and subcellular distribution of radionuclides. *J Nucl Med.* 1994;35:521–530.
28. Howell RW. Radiation spectra for Auger electron emitting radionuclides: Report No. 2 of AAPM Nuclear Medicine Task Group No. 6. *Med Phys.* 1992;19:1371–1383.
29. Hubbel JH. Photon mass attenuation and energy absorption coefficients from 1 keV to 20 MeV. *Int J Appl Radiat Isot.* 1982;33:1269–1290.
30. Howell RW, Rao DV, Sastry KSR. Macroscopic dosimetry for radioimmunotherapy: nonuniform activity distributions in solid tumors. *Med Phys.* 1989;16:66–74.
31. Eckerman KF, Westfall RJ, Ryman JC, Cristy M. *Nuclear Decay Data Files of the Dosimetry Research Group*. ORNI/TM-12350. Knoxville, TN: Oak Ridge National Laboratory; 1993.
32. ICRU. *Stopping Powers for Electrons and Positrons: Report 37*. Bethesda, MD: International Commission on Radiation Units and Measurements; 1984.
33. Goddu SM, Howell RW, Rao DV. A generalized approach to absorbed dose calculations for dynamic tumor and organ masses. *J Nucl Med.* 1995;36:1923–1927.
34. Howell RW, Narra VR, Rao DV. Absorbed dose calculations for rapidly growing tumors. *J Nucl Med.* 1992;33:277–281.
35. Waterman FM, Yue N, Corn BW, Dicker AP. Edema associated with I-125 or Pd-103 prostate brachytherapy and its impact on post-implant dosimetry: an analysis based on serial CT acquisition. *Int J Radiat Oncol Biol Phys.* 1999;43:447–454.
36. McCarthy KE, Woltering EA, Epenan GD, et al. In situ radiotherapy with ^{111}In-pentreotide: initial observations and future directions. *Cancer J Sci Am.* 1998;4:94–102.
37. Krenning EP, Kooij PPM, Bakker WH, et al. Radiotherapy with a radiolabeled somatostatin analogue, [^{111}In-DTPA-D-Phe^{1}]-Octreotide: a case history. *Ann N Y Acad Sci.* 1993;733:496–506.

snm advancing molecular imaging

Downloaded from jnm.snmjournals.org by on March 14, 2017. For personal use only.

JNM The Journal of NUCLEAR MEDICINE

Role of Lipid-Soluble Complexes in Targeted Tumor Therapy

Mathew L. Thakur, Ron Coss, Roger Howell, Donka Vassileva-Belnikolovska, Jeff Liu, Sampath P. Rao, Greg Spana, Phyllis Wachsberger and Dennis L. Leeper

J Nucl Med. 2003;44:1293-1300.

This article and updated information are available at:
http://jnm.snmjournals.org/content/44/8/1293

Information about reproducing figures, tables, or other portions of this article can be found online at:
http://jnm.snmjournals.org/site/misc/permission.xhtml

Information about subscriptions to JNM can be found at:
http://jnm.snmjournals.org/site/subscriptions/online.xhtml

The Journal of Nuclear Medicine is published monthly.
SNMMI | Society of Nuclear Medicine and Molecular Imaging
1850 Samuel Morse Drive, Reston, VA 20190.
(Print ISSN: 0161-5505, Online ISSN: 2159-662X)

© Copyright 2003 SNMMI; all rights reserved.

SNMMI SOCIETY OF NUCLEAR MEDICINE AND MOLECULAR IMAGING